

Experimental validation of the $1/\tau$ -scaling entropy generation in finite-time thermodynamics with dry air

Yu-Han Ma,^{1,2} Ruo-Xun Zhai,^{3,2} Chang-Pu Sun,^{1,2} and Hui Dong^{2,*}

¹Beijing Computational Science Research Center, Beijing 100193, China

²Graduate School of China Academy of Engineering Physics,

No. 10 Xibeiwang East Road, Haidian District, Beijing, 100193, China

³Beijing Normal University, Beijing 100875, China

The second law of thermodynamics can be described as the non-decreasing of the entropy in the irreversible thermodynamic process. Such phenomenon can be quantitatively evaluated with the irreversible entropy generation (IEG), which was recently found to follow a $1/\tau$ scaling for the system under a long contact time τ with the thermal bath. This scaling, predicted in many finite-time thermodynamic models, is of great potential in the optimization of heat engines, yet remains lack of direct experimental validation. In this letter, we design an experimental apparatus to test such scaling by compressing dry air in a temperature-controlled water bath. More importantly, we quantitatively verify the optimized control protocol to reduce the IEG. Such optimization shall bring new insight to the practical design of heat engine cycles.

Introduction- Heat engines, converting heat into useful work, have important practical applications and attract a wide range of research interests in both classical and quantum thermodynamics [1–6]. In classical thermodynamics, the Carnot theorem [1] limits the maximum efficiency of heat engines with the well-know Carnot efficiency $\eta_C = 1 - T_c/T_h$, where $T_c(T_h)$ is temperature for the cold (hot) bath. Unfortunately, achieving such efficiency is typically accompanied by a vanishing output power due to the infinite long operation time in a quasi-static thermodynamic process [1, 7–10]. The futility of such heat engine with vanishing power has pushed to design finite-time cycle to achieve high efficiency while maintaining the output power [11–16]. For such design, the quantitative evaluation of the irreversibility is the key for optimization [6, 11, 14–20]. The trade-off relation between power and efficiency [21–24] are significantly determined by the relation of irreversible entropy generation (IEG) on the control time τ . In the near-equilibrium region, the IEG in a finite-time isothermal process is found inversely proportional to the process time τ , namely the \mathcal{C}/τ scaling with the coefficient \mathcal{C} . Such scaling has been discovered in different finite-time thermodynamic models [25], such as endo-reversible model [11, 12, 26, 27], linear model [14, 19, 28, 29], stochastic model [30–34], and low-dissipation model [16, 24, 35]. Moreover, the scaling relation has been established not only for the classical working substance [12], but also for quantum working substance [23, 24, 36]. The coefficient \mathcal{C} is determined by the statistical properties of the working substance and the heat bath, and has recently been proved to be related to the way that the working substance being manipulated [36, 37].

To our best knowledge, the direct verification of the \mathcal{C}/τ scaling was rarely explored, although the behavior of finite-time heat engines has been studied in several experimental platforms [39–46]. In this letter, we focus on experimental measuring IEG of dry air via the work done

in the finite-time isothermal process with designed apparatus, and reveal the impact of control scheme on the IEG quantitatively. In order to validate the \mathcal{C}/τ scaling, a controlled apparatus in Fig. 1(a) is designed to measure the state of the dry air, which is sealed in a compressible cylinder (A) and three buffer cylinders (B, C, D), immersed in a temperature-controlled water bath. A piston is installed in the cylinder A to compress the air with a computer-controlled stepper motor M. By setting different push programs, a controllable change in the volume of the gas over time is achieved, i.e., $V(t) = V_0 - \mathcal{A}L(t)$, where $V_0 = 2.584 \times 10^{-3} \text{m}^3$ is the initial volume of the gas, and $\mathcal{A} = 1.963 \times 10^{-2} \text{m}^2$ is the cross sectional area of the cylinder A. The current setup allows us to realize the finite-time isothermal process with different process time τ .

We firstly sketch the origin of the \mathcal{C}/τ scaling for a general classic system, which contacts with a heat bath of constant temperature T_e . A control parameter, e.g., the volume V of the gas, is tuned from $t = 0$ to the end of the process $t = \tau$. In this process, with the endo-reversible assumption [11, 12, 26, 27], IEG is written as [12]

$$\Delta S^{(\text{ir})} = \int_0^\tau \left(\frac{dQ_s}{T_s} + \frac{dQ_e}{T_e} \right), \quad (1)$$

where $dQ_s = -dQ_e$ is the heat absorbed by the system from the heat bath. The effective temperature T_s of the system generally varies with time in the control process. In the condition of the quasi-static process with infinite control time ($\tau \rightarrow \infty$), the system is always in the thermal equilibrium with $T_s = T_e$. For the long time τ in comparison to the relaxation time t_r between the gas and the heat bath, the system is in the linear irreversible region, such that T_s is slightly deviated from the bath temperature, namely $|T_s - T_e|/T_e \ll 1$. The heat exchange rate between the system and bath follows the Newton's law of cooling as

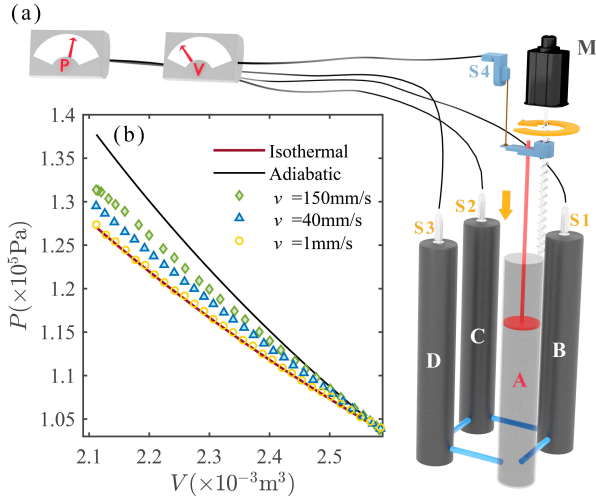


Figure 1. Experimental setup for measuring irreversible entropy generation in the finite-time isothermal process. (a) Experimental setup. The dry air is sealed in four connected cylinders A, B, C, and D. The piston of A is propelled by the computer-controlled stepper motor M to achieve the controlled compression of the gas. Three pressure sensors S1, S2, and S3 are connected to the top of the three cylinders B, C, and D respectively to measure the air pressure in the cylinders $P(t)$. And the displacement of the piston $L(t)$ is detected by a position sensor S4 to reveal the gas volume V . The cylinders are immersed in the water bath with adjustable temperature. (b) $P - V$ diagram of the gas under the bath temperature $T_e = 313.15\text{K}$ is illustrated in figure (b). The green diamonds, blue triangles, and yellow circles are obtained for the piston speeds 150mm/s, 40mm/s, and 1mm/s, respectively. The red solid line shows the theoretical quasi-static isothermal process, namely, $PV = \text{const}$, and the black solid line represents the adiabatic process with $PV^\gamma = \text{const}$. Here, $\gamma = 1.4$ is the heat capacity ratio of the dry air [38].

$$\frac{dQ_s}{dt} = -\kappa(T_s - T_e), \quad (2)$$

where κ is the thermal conductance. Combining Eqs. (1) and (2), we obtain IEG as

$$\Delta S^{(\text{ir})} = \frac{\int_0^1 J^2 d\tilde{t}}{\kappa T_e^2 \tau}, \quad (3)$$

where $J = dQ_s/d\tilde{t}$ is the heat flux, and $\tilde{t} = t/\tau$ is the normalized time. The above equation shows the origin of $1/\tau$ scaling for the IEG.

For the current dry air system with volume compressed from V_0 to V_f , the IEG is found proportional to the irreversible work $W^{(\text{ir})}$ (IW) in the process under the long time limit as follow

$$W^{(\text{ir})} = T_e \Delta S^{(\text{ir})} = \frac{P_0^2 (V_f - V_0)^2}{\kappa T_e \tau}, \quad (4)$$

where P_0 is the initial pressure of the dry air. The irreversible work $W^{(\text{ir})}(\tau) = W(\tau) - W_q$ is obtained by subtracting the work $W_q = P_0 V_0 \ln(V_0/V_f)$ in the quasi-static isothermal process from the work $W(\tau) = -\int_0^\tau P dV$ in the finite-time isothermal process. The detail of the current derivation is shown in the Supplementary Materials. We will characterize the irreversibility of the current system via the irreversible work, which is a directly measurable quantity [12, 17] in our current setup.

Verification of $1/\tau$ scaling - To measure the work $W(\tau)$, we monitor the pressure $P = P(t)$ with three sensors, numbered S1, S2 and S3 (range 0-0.15Mpa, accuracy 0.1%) on the top of the three cylinders B, C, and D respectively. The volume change $dV = \mathcal{A}dL(t)$ is measured through the piston position $L(t)$ with the sensor S4 (range 0-0.3m, accuracy 0.1%).

In the whole compression process, the four cylinders are immersed in a large water bath (volumn 100L) with controllable temperature (accuracy 0.5K). The internal equilibrium time of the gas is much smaller than the relaxation time t_r that the gas is always in the equilibrium state with temperature T_s , known as the endo-reversible [11, 12, 26, 27]. In the current setup, $t_r = 1.942\text{s}$ is measured in the experiment with details explained in the Supplementary Materials.

The state of the dry air is illustrated via the P - V diagram in Fig. 1(b). The pressure $P(t)$ is obtained from the sensor S1 and the volume is measured by $V(t) = V_0 - \mathcal{A}L(t)$ with $L(t)$ from the sensor S4. The total displacement of the piston is $\Delta L = L(\tau) = 240\text{mm}$. The sample frequency for all sensors is set as 50Hz. In the plot, we show the P - V diagram for the different piston speeds v , 150mm/s (green diamond), 40mm/s (blue triangle), and 1mm/s (yellow circle). It can be seen from Fig. 1(b) that the slower the pushing speed, the closer the curve is to the quasi-static isothermal process, as shown by the red solid line. Conversely, the less heat exchange between the gas and the heat bath for the fast push, and the $P - V$ curve is closer to the adiabatic process marked with the black solid line ($PV^\gamma = \text{const}$). Here $\gamma = 1.4$ is the heat capacity ratio for dry air [38]. The data from pressure sensors S2 and S3 are illustrated in Supplementary Materials.

By integrating the $P - V$ curve, we obtain the work done by the piston to the gas as

$$W(\tau) = - \int_0^\tau P(t) \dot{V}(t) dt. \quad (5)$$

The work as the function of the process time τ is illustrated in Fig. 2(a), where the red circle and blue diamond are obtained by setting the bath temperature $T_e=323.15\text{K}$ and $T_e=313.15\text{K}$ respectively. Fig. 2(a) shows that the work approaches a stable value, which matches the work in the quasi-static isothermal process W_q (the dash-dotted line). As shown with the log-log plot

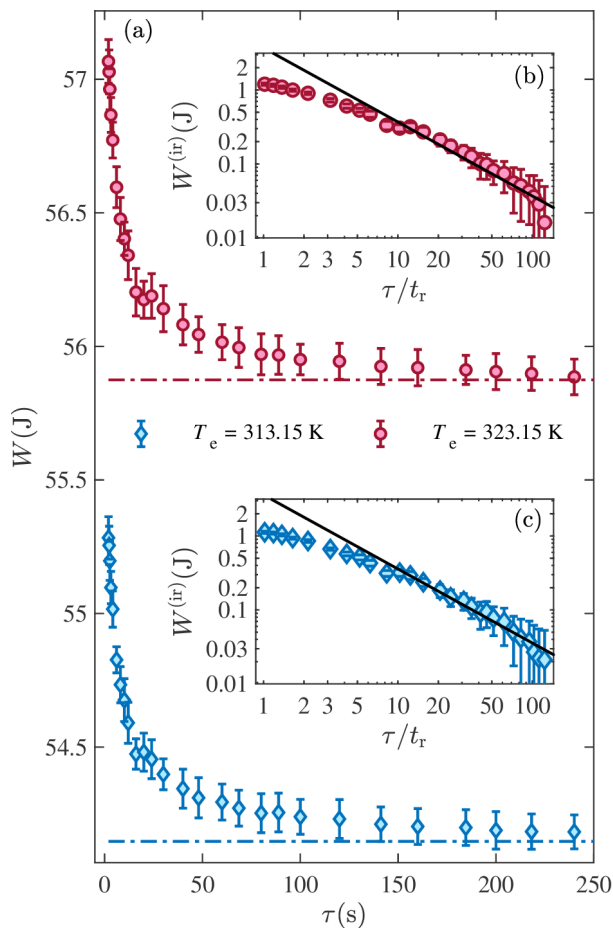


Figure 2. Work in the finite time isothermal process. (a) Work done by the piston on the gas as the function of the process time τ . The experimental results are illustrated by the red circled and blue diamond with the corresponding bath temperature $T_e = 323.15\text{K}$ and $T_e = 313.15\text{K}$ respectively. The work W_q in the quasi-static process is marked by the red (blue) dash-dotted line for $T_e = 323.15\text{K}$ (313.15K). The log-log plot of the irreversible work $W^{(ir)}$ as the function of dimensionless time τ/t_r is illustrated in (b) with $T_e = 323.15\text{K}$ and (c) with $T_e = 313.15\text{K}$. The corresponding theoretical result of Eq. (4) is represented by the black solid line.

of the IW in Fig. 2(b) and (c), in the long time region of $\tau \gg t_r$, the experimental obtained IW is in good agreement with the theoretical prediction of Eq. (3), which is represented by the black solid line. Therefore, we validate the behavior that the IEG is inversely proportional to the process time in the long-time region.

Effect of the control scheme - With the above compression process at the constant speed, we have validated the $1/\tau$ scaling of the IEG via the measurement of the IW. As predicted in the previous study [12, 36], the coefficient in the $1/\tau$ scaling relation of IW not only is determined by the system parameters of the working substance and heat bath, but also relates to the specific way how the state of the working substance is tuned. In the following

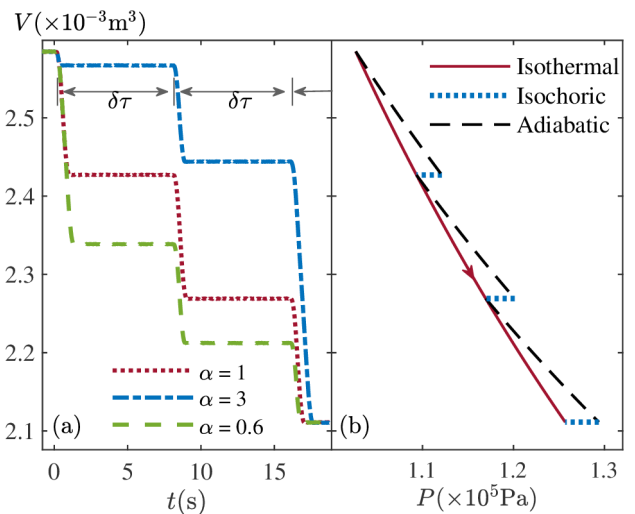


Figure 3. The volume change and the $P - V$ diagram in the discrete isothermal process with the 3-step case as an example. (a) Volume changes with time in the 3-step DIP with different push modes, where the step time is $\delta\tau = 8\text{s}$. The piston is pushed with $L_i = (i/3)^\alpha \Delta L$, ($i = 1, 2, 3$), where L_i is the displacement of the piston after the end of the i -th step. The gas volume $V_i = V_0 - \mathcal{A}L_i$ being tuned sub-linearly ($\alpha = 0.6$), linearly ($\alpha = 1$), and super-linearly ($\alpha = 3$) are illustrated by the green dashed line, red dotted line, and blue dash-dotted line respectively. (b) P - V diagram of the 3-step DIP. Series of adiabatic (black dashed line) and isochoric (blue dotted line) processes are used to approach a finite-time isothermal process (red solid line). In the i -th ($i = 1, 2, 3$) step, the gas volume is firstly compressed from V_i to V_{i+1} adiabatically, then the gas isochorically relaxes to the thermal equilibrium state with the same temperature T_e as the water bath. The experimental $P - V$ diagram is shown in the Supplementary Materials.

experiment, we will show the impact of different control schemes on IW with our setup via a discrete isothermal process [17].

The discrete isothermal process, introduced by Andresen et al. in Ref. [47], is an effective approach to optimize the finite-time Carnot engine. Since then, the discrete step thermodynamic process have also been used to study of different thermodynamic issues, such as work distribution [48], thermodynamic length [49], and optimization of quantum heat engines [36, 50]. The basic idea of the discrete step isothermal process (DIP) is to use a series of adiabatic and isochoric processes to construct a finite-time isothermal process. The discrete isothermal process has two obvious advantages, theoretically the state of the working substance can be analytically solved and experimentally the work and the heat exchange are separated for direct measurement.

In our setup, the piston is rapidly pushed in the i -th step to the position L_i ($i = 1, 2, \dots, M$) to form an adiabatic process, and then relaxes to thermal equilibrium through the isochoric process with duration $\delta\tau$,

as shown in Fig. 3(a). The initial (final) piston position is $L_0 = 0$ ($L_M = \Delta L$). For clarity, we show three control schemes with different α with total step number $M = 3$ and duration time $\delta\tau = 8$ s as an example. At the beginning of the each adiabatic process, the gas maintains the same temperature as the water bath, since $\delta\tau$ is larger than the relaxation time t_r that $\exp[-\delta\tau/t_r] \ll 1$. We define the average speed of the piston in one step as $v_i = (L_i - L_{i-1})/\delta\tau$. The stepper motor can be set to push the piston L_i with a power function $L_i = (i/M)^\alpha \Delta L$ in the i -th step.

For the discrete isothermal process involving $M \gg 1$ steps, the IW of the system is explicitly written as [See Supplementary Materials for detailed derivation]

$$W^{(\text{ir})} = \frac{\Lambda\Theta}{M}, \quad (6)$$

where $\Theta = (\gamma - 1) P_0 (V_f - V_0)^2 / (2V_0)$ relates to the initial and final state of the system. And $\Lambda = \langle v^2 \rangle / \langle v \rangle^2$, characterizing the speed fluctuation of the piston, is determined by the control scheme of the stepper motor with $\langle v^2 \rangle \equiv \sum_{i=1}^M v_i^2 / M$ and $\langle v \rangle = \sum_{i=1}^M v_i / M$. The current general formula in Eq. (6) recovers the result for piston compressed with the constant speed noticing $\Lambda = 1$. With the fixed process time $\tau = M\delta\tau$, any control scheme under power function [36] results in the larger $\Lambda > 1$, which in turn induces the larger IW $W^{(\text{ir})}$ than that with the constant speed.

With the current setup, we can experimentally demonstrate the effect of the control function on the IW. The control functions are realized by the different power indexes α . The volume change of the gas in a 3-step DIP is illustrated in Fig. 3(a), where the green dashed line, red dotted line, and blue dash-dotted line relate to the piston been pushed sub-linearly, linearly, and super-linearly, respectively. The schematic $P - V$ curve for the DIP is illustrated in Fig. 3(b).

The irreversible work done in DIP is obtained by integrating area under the P-V curve, and illustrated in Fig. 4(a) as a function of the total step number M for three different power indexes $\alpha = 0.6$ (green triangle), 1.0 (red circle) and 3.0 (blue diamond). Each data points have been averaged with 20 repeats. The corresponding dashed lines show the fitting with the theoretical result in Eq. (6). At the large- M region, the IW is inversely proportional to M , namely, inversely proportional to the total time τ .

To show the dependence of the IW on the control function, we plot the coefficient Λ of the $1/M$ scaling in Eq. (6) as a function of the index α in Fig. 4(b). The experimental data for coefficient Λ , shown as diamonds in Fig. 4(b), is obtained by fitting curves in 4(a) with Eq. (6) for different α at large step number M . The theoretical result of Eq. (6) is shown as the green circle in Fig. 4. The figure shows the agreement between the theoretical

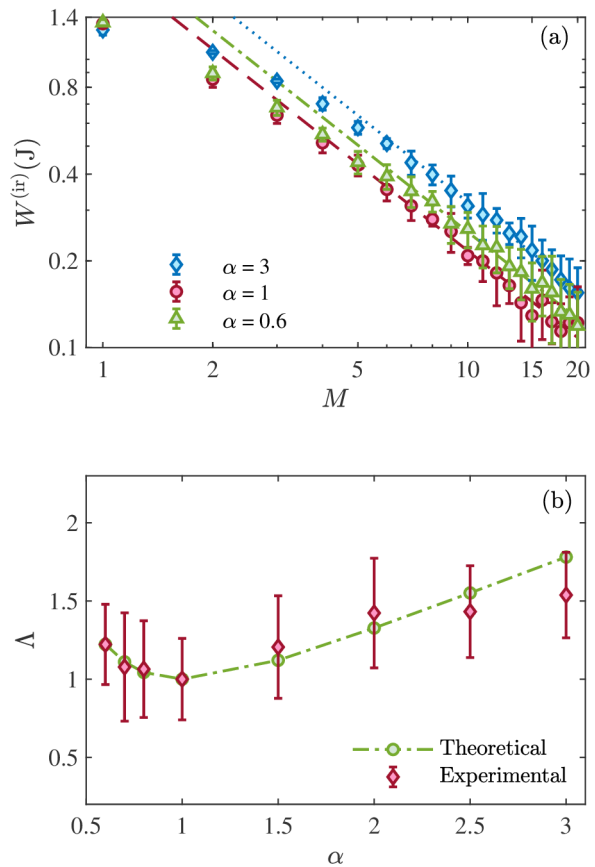


Figure 4. Irreversible work with different piston push schemes of the discrete isothermal process. The temperature of the water bath is $T_e = 313.15\text{K}$. (a) log-log plot of irreversible work as the function of step number M . We demonstrate the $1/M$ scaling for three control functions with $\alpha = 3$ (the blue diamond), 0.6 (green triangle), and 1 (red circle). (b) The obtained parameter Λ in Eq. (6) as the function of power index α . The experiment results, represented by the red diamond, are obtained by fitting the relation of $W^{(\text{ir})} \sim 1/M$. The theoretical curve in Eq. (6) is plotted with the green dash-dotted line as a comparison.

result and the experimental data. The experimental data shows a minimum irreversible work at $\alpha = 1$. We conclude that within the set of power function, the minimal IW is achieved with the linearly control function [36], namely $\alpha = 1$ as shown in Fig. 4.

With the dependence of the control function Λ , we can control the IW of the system by different schemes of compression to adjust the power and efficiency of the heat engine [36]. Experimentally, such tuning of irreversible entropy generation via adjusting the mode of operation is meaningful for the design of heat engine with high output power and efficiency.

Conclusion—We have designed the apparatus with the cylinder-gas system to validate the theoretically predicted $1/\tau$ scaling of irreversible entropy generation in the finite-time thermodynamics. Our experiment for the

first time directly shows that the irreversible entropy generation, obtained by measuring the irreversible work, is inversely proportional to the process time τ in the long-time region [Fig. 2(b)], namely, $\Delta S^{(ir)} \propto 1/\tau$. More importantly, we demonstrated the proportional relationship between IEG and the speed fluctuation of the piston in different gas compression schemes for the discrete isothermal process. Specifically, we verified the minimal IEG can be achieved by pushing the piston linearly within the set of the power control functions. This provides a feasible and convenient solution for the optimization of the actual heat engine by applying different control schemes to the work substance in different processes of the thermodynamic cycle.

The similar detection of the irreversible work can also be realized in quantum system, such as trapped ions [40, 45, 51], NMR system [52] and superconducting circuit systems [53, 54]. The generalization of the current measurement in quantum regime could potentially shows the influence of coherence on these thermodynamic quantities [55–57].

Yu-Han Ma is grateful to Hong Yuan and Jin-Fu Chen for helpful discussions. This work is supported by the NSFC (Grants No. 11534002 and No. 11875049), the NSAF (Grant No. U1730449 and No. U1530401), and the National Basic Research Program of China (Grants No. 2016YFA0301201 and No. 2014CB921403). H.D. also thanks The Recruitment Program of Global Youth Experts of China.

* hdong@gcsaep.ac.cn

- [1] K. Huang, *Introduction To Statistical Physics, 2Nd Edition* (T&F/Crc Press, 2013), ISBN 978-1-4200-7902-9.
- [2] M. Esposito, U. Harbola, and S. Mukamel, *Rev. Mod. Phys.* **81**, 1665 (2009).
- [3] M. Campisi, P. Hänggi, and P. Talkner, *Rev. Mod. Phys.* **83**, 771 (2011).
- [4] J. P. Pekola, *Nat. Phys.* **11**, 118 (2015).
- [5] S. Vinjanampathy and J. Anders, *Contemp. Phys.* **57**, 545 (2016).
- [6] F. Binder, L. A. Correa, C. Gogolin, J. Anders, and G. Adesso, eds., *Thermodynamics in the Quantum Regime* (Springer International Publishing, 2018).
- [7] C. M. Bender, D. C. Brody, and B. K. Meister, *J. Phys. A: Math. Theor.* **33**, 4427 (2000).
- [8] T. E. Humphrey, R. Newbury, R. P. Taylor, and H. Linke, *Phys. Rev. Lett.* **89**, 116801 (2002).
- [9] H. T. Quan, Y. xi Liu, C. P. Sun, and F. Nori, *Phys. Rev. E* **76**, 031105 (2007).
- [10] Y.-H. Ma, S.-H. Su, and C.-P. Sun, *Phys. Rev. E* **96**, 022143 (2017).
- [11] F. L. Curzon and B. Ahlborn, *Am. J. Phys.* **43**, 22 (1975).
- [12] P. Salamon, A. Nitzan, B. Andresen, and R. S. Berry, *Phys. Rev. A* **21**, 2115 (1980).
- [13] K. Sekimoto and S. ichi Sasa, *J. Phys. Soc. Jpn* **66**, 3326 (1997).
- [14] C. V. den Broeck, *Phys. Rev. Lett.* **95**, 190602 (2005).
- [15] Z. C. Tu, *J. Phys. A: Math. Theor.* **41**, 312003 (2008).
- [16] M. Esposito, R. Kawai, K. Lindenberg, and C. V. den Broeck, *Phys. Rev. Lett.* **105**, 150603 (2010).
- [17] B. Andresen, P. Salamon, and R. S. Berry, *Physics today* p. 63 (1984).
- [18] J. Chen, *J. Phys. D Appl. Phys.* **27**, 1144 (1994).
- [19] A. Ryabov and V. Holubec, *Phys. Rev. E* **93**, 050101 (2016).
- [20] V. Holubec and A. Ryabov, *Phys. Rev. E* **96**, 062107 (2017).
- [21] V. Holubec and A. Ryabov, *J. Stat. Mech.: Theory E.* **2016**, 073204 (2016).
- [22] N. Shiraishi, K. Saito, and H. Tasaki, *Phys. Rev. Lett.* **117**, 190601 (2016).
- [23] V. Cavina, A. Mari, and V. Giovannetti, *Phys. Rev. Lett.* **119**, 050601 (2017).
- [24] Y.-H. Ma, D. Xu, H. Dong, and C.-P. Sun, *Phys. Rev. E* **98**, 042112 (2018).
- [25] Z.-C. Tu, *Chin. Phys. B* **21**, 020513 (2012).
- [26] M. H. Rubin, *Phys. Rev. A* **19**, 1272 (1979).
- [27] B. Sahin, A. Kodali, and H. Yavuz, *Energy* **21**, 1219 (1996).
- [28] Y. Wang and Z. C. Tu, *Phys. Rev. E* **85**, 011127 (2012).
- [29] J. Stark, K. Brandner, K. Saito, and U. Seifert, *Phys. Rev. Lett.* **112**, 140601 (2014).
- [30] I. Derényi and R. Astumian, *Phys. Rev. A* **59**, R6219 (1999).
- [31] T. Schmiedl and U. Seifert, *EPL (Europhysics Letters)* **81**, 20003 (2007).
- [32] Y. Izumida and K. Okuda, *EPL (Europhysics Letters)* **83**, 60003 (2008).
- [33] U. Seifert, *Rep. Prog. Phys* **75**, 126001 (2012).
- [34] A. Dechant, N. Kiesel, and E. Lutz, *Phys. Rev. Lett.* **114**, 183602 (2015).
- [35] C. de Tomás, A. C. Hernández, and J. M. M. Roco, *Phys. Rev. E* **85**, 010104 (2012).
- [36] Y.-H. Ma, D. Xu, H. Dong, and C.-P. Sun, *Phys. Rev. E* **98**, 022133 (2018).
- [37] Z. Gong, Y. Lan, and H. T. Quan, *Physical Review Letters* **117**, 180603 (2016).
- [38] D. E. Krause and W. J. Keeley, *Phys. Teach.* **42**, 481 (2004).
- [39] V. Blickle and C. Bechinger, *Nat. Phys.* **8**, 143 (2011).
- [40] O. Abah, J. Roßnagel, G. Jacob, S. Deffner, F. Schmidt-Kaler, K. Singer, and E. Lutz, *Phys. Rev. Lett.* **109**, 203006 (2012).
- [41] J.-P. Brantut, C. Grenier, J. Meineke, D. Stadler, S. Krimmer, C. Kollath, T. Esslinger, and A. Georges, *Science* **342**, 713 (2013).
- [42] J. Roßnagel, O. Abah, F. Schmidt-Kaler, K. Singer, and E. Lutz, *Phys. Rev. Lett.* **112**, 030602 (2014).
- [43] J. Gieseler, R. Quidant, C. Dellago, and L. Novotny, *Nat. Nanotechnol* **9**, 358 (2014).
- [44] I. A. Martínez, É. Roldán, L. Dinis, D. Petrov, J. M. R. Parrondo, and R. A. Rica, *Nat. Phys.* **12**, 67 (2015).
- [45] J. Rosnagel, S. T. Dawkins, K. N. Tolazzi, O. Abah, E. Lutz, F. Schmidt-Kaler, and K. Singer, *Science* **352**, 325 (2016).
- [46] S. Deng, A. Chenu, P. Diao, F. Li, S. Yu, I. Coulamy, A. del Campo, and H. Wu, *Sci. Adv.* **4**, eaar5909 (2018).
- [47] B. Andresen, R. S. Berry, A. Nitzan, and P. Salamon, *Phys. Rev. A* **15**, 2086 (1977).
- [48] H. T. Quan, S. Yang, and C. P. Sun, *Phys. Rev. E* **78**,

- 021116 (2008).
- [49] G. E. Crooks, Phys. Rev. Lett. **99**, 100602 (2007).
 - [50] E. Geva and R. Kosloff, J. Chem. Phys. **96**, 3054 (1992).
 - [51] S. An, J.-N. Zhang, M. Um, D. Lv, Y. Lu, J. Zhang, Z.-Q. Yin, H. Quan, and K. Kim, Nat. Phys. **11**, 193 (2015).
 - [52] R. J. de Assis, T. M. de Mendonça, C. J. Villas-Boas, A. M. de Souza, R. S. Sarthour, I. S. Oliveira, and N. G. de Almeida, Phys. Rev. Lett. **122**, 240602 (2019).
 - [53] F. Giazotto, T. T. Heikkilä, A. Luukanen, A. M. Savin, and J. P. Pekola, Rev. Mod. Phys. **78**, 217 (2006).
 - [54] R. Uzdin and N. Katz, arXiv:1908.08968 (2019).
 - [55] K. Brandner, M. Bauer, and U. Seifert, Phys. Rev. Lett. **119**, 170602 (2017).
 - [56] S. Su, J. Chen, Y. Ma, J. Chen, and C. Sun, Chin. Phys. B **27**, 060502 (2018).
 - [57] P. A. Camati, J. F. G. Santos, and R. M. Serra, Phys. Rev. A **99**, 062103 (2019).

Supplementary Materials to “Experimental validation of the $1/\tau$ -scaling entropy generation in finite-time thermodynamics with dry air”

Yu-Han Ma,^{1,2} Ruo-Xun Zhai,^{3,2} Chang-Pu Sun,^{1,2} and Hui Dong^{2,*}

¹Beijing Computational Science Research Center, Beijing 100193, China

²Graduate School of China Academy of Engineering Physics,

No. 10 Xibeiwang East Road, Haidian District, Beijing, 100193, China

³Beijing Normal University, Beijing 100875, China

This document is devoted to providing the detailed derivations and the supporting discussions to the main content in the Letter.

I. IRREVERSIBLE ENTROPY GENERATION AND IRREVERSIBLE WORK OF DRY AIR

In this section we derive the relation between the irreversible work and the irreversible entropy generation for the current system with dry air. The irreversible entropy generation is generally defined as

$$\Delta S^{(\text{ir})} = \int_0^\tau \left(\frac{dQ}{T_s} - \frac{dQ}{T_e} \right) \quad (\text{S1})$$

$$= \int_0^\tau \frac{dU + PdV}{T_s} - \frac{1}{T_e} \int_0^\tau (dU + PdV) \quad (\text{S2})$$

$$= \int_0^\tau \frac{C_V dT + \frac{nRT_s}{V} dV}{T_s} - \frac{1}{T_e} \int_0^\tau (C_V dT + PdV) \quad (\text{S3})$$

$$= C_V \ln \left(\frac{T_s(\tau)}{T_e} \right) - C_V \frac{T_s(\tau) - T_e}{T_e} - \frac{\int_0^\tau PdV}{T_e} + nR \ln \left(\frac{V_f}{V_0} \right). \quad (\text{S4})$$

Under the long time limit with $|T_s - T_e|/T_e \ll 1$, the irreversible entropy generation $\Delta S^{(\text{ir})}$ is simplified to the first order of $(T_s - T_e)/T_e$ as

$$\Delta S^{(\text{ir})} = \frac{W - W_q}{T_e}, \quad (\text{S5})$$

where $W(\tau) = -\int_0^\tau PdV$ is the total work done by the piston to the gas during the finite-time process and $W_q = nRT_e \ln(V_0/V_f)$ is the work done for quasi-static process. Here, n is the number of moles and R is the ideal gas constant. The irreversible work is defined as $W^{(\text{ir})} = W - W_q$, which is connected to the entropy generation via

$$W^{(\text{ir})} = T_e \Delta S^{(\text{ir})}. \quad (\text{S6})$$

This simplification allows the direct measurement of the irreversibility via irreversible work $W^{(\text{ir})}$ in the current setup.

II. MEASURE THE RELAXATION TIME t_r

In the data analysis, the relaxation time t_r can be directly determined via the relaxation process. During the isochoric process with the pressure relaxation, the change of the internal energy of the gas is caused by the heat exchange

$$\frac{dU}{dt} = \frac{dQ_s}{dt} = -\kappa(T_s - T_e). \quad (\text{S7})$$

Combining with internal energy equation $dU = C_V dT$, we have the explicit evolution of the temperature as

$$T_s(t) = T_e + [T_s(0) - T_e] e^{-t/t_r}, \quad (\text{S8})$$

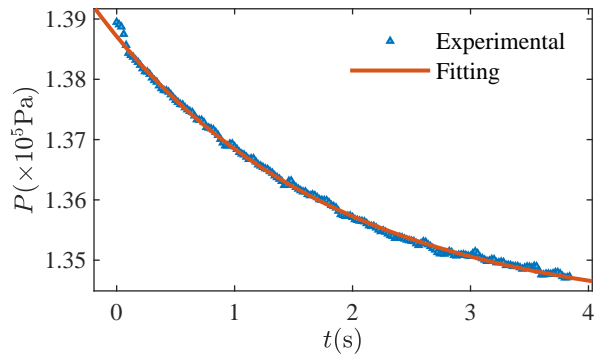


Figure S1. The pressure change after the fast compression. The blue triangles show the experimental data from pressure sensor S1, and the red line illustrates the fitting with the curve in Eq. (S9). The relaxation time $t_r = 1.942\text{s}$ is obtained by fitting the experimental data.

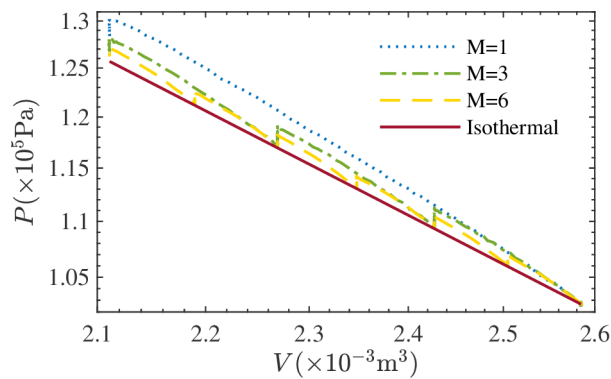


Figure S2. $P - V$ diagram of the gas in discrete isothermal process. $P - V$ diagram with different step number M . The blue dotted line, green dash-dotted line, and yellow dashed line relates to $M = 1$, $M = 3$, and $M = 6$, respectively. The isothermal line of the gas is illustrated by the red solid line.

where, $t_r = C_V/\kappa$ is the relaxation time. The dynamical change of the temperature is directly reflected through the change of the pressure via the ideal gas equation as $P(t) = nRT_s(t)$. To measure the relaxation time, we compress the sealed gas with the maximum speed to the final volume V_f , and measure the pressure change $P(t)$. The measured data, shown in Fig. S1, is fitted with the curve

$$P(t) = \frac{nR}{V} [T_e + [T_s(0) - T_e] e^{-t/t_r}]. \quad (\text{S9})$$

The experimental fitting results in the relaxation time $t_r = 1.942\text{s}$.

III. IRREVERSIBLE ENTROPY GENERATION IN DISCRETE ISOTHERMAL PROCESS

In this section, we provide the detailed derivation of Equation (6) in the letter. The discrete isothermal process (DIP) consisting of a series of adiabatic processes and isochoric processes is used to approach the quasi-static isothermal process. The experimental obtained $P - V$ diagram of the gas in DIP with different step number M are illustrated in Fig. S2.

The work done by the piston to the gas in the i -th step comes only from the i -th adiabatic process as

$$W_i = - \int_{V_{i-1}}^{V_i} P_i(V) dV, \quad (\text{S10})$$

where the pressure follows the adiabatic equation of idea gas as

$$P_i(V) = \frac{P_i^0 V_{i-1}^\gamma}{V^\gamma}, V \in [V_{i-1}, V_i], \quad (\text{S11})$$

where $\gamma = C_P/C_V$ is the heat capacity ratio of the gas. Initially at i -th adiabatic step, the gas is in equilibrium with the bath i.g., $T_i = T_e$. And the pressure is $P_i^0 = nk_B T_i/V_{i-1}$. The work done at the i -th adiabatic process is obtained explicitly by integration,

$$W_i = - \int_{V_{i-1}}^{V_i} \frac{P_i^0 V_{i-1}^\gamma}{V^\gamma} dV = \frac{nRT_e}{1-\gamma} \left[\left(\frac{V_i}{V_{i-1}} \right)^{1-\gamma} - 1 \right]. \quad (\text{S12})$$

And the total work is the summation over all the adiabatic process

$$\Delta W = \sum_{i=1}^M W_i = - \frac{nRT_e}{1-\gamma} \sum_{i=1}^M \left[\left(\frac{V_i}{V_{i-1}} \right)^{1-\gamma} - 1 \right]. \quad (\text{S13})$$

A similar result was reported in Ref. [S1], where the authors used isobaric processes instead of adiabatic processes.

The volume of the sealed gas is controlled by the piston via the function

$$V_i = V_0 - \mathcal{A}L_i, \quad (\text{S14})$$

where \mathcal{A} is the cross section of the piston. With the control, the work for each adiabatic process of Eq. (S12) becomes

$$W_i = - \frac{nRT_e}{1-\gamma} \left[\left(\frac{V_0 - \mathcal{A}L_i}{V_0 - \mathcal{A}L_{i-1}} \right)^{1-\gamma} - 1 \right] \quad (\text{S15})$$

$$= - \frac{nRT_e}{1-\gamma} \left[\left(1 + \frac{L_{i-1} - L_i}{V_0/\mathcal{A} - L_{i-1}} \right)^{1-\gamma} - 1 \right] \quad (\text{S16})$$

$$\approx - \frac{nRT_e}{1-\gamma} \left[(1-\gamma) \frac{L_{i-1} - L_i}{V_0/\mathcal{A} - L_{i-1}} - \frac{\gamma(1-\gamma)}{2} \left(\frac{L_{i-1} - L_i}{V_0/\mathcal{A} - L_{i-1}} \right)^2 \right] \quad (\text{S17})$$

$$= \frac{nRT_e v_i \delta\tau}{V_0/\mathcal{A} - L_{i-1}} + \frac{\gamma nRT_e}{2} \left(\frac{v_i \delta\tau}{V_0/\mathcal{A} - L_{i-1}} \right)^2, \quad (\text{S18})$$

where $v_i \equiv (L_i - L_{i-1})/\delta\tau$ is the average speed of the piston in the i -th step. Then, by keeping up to the second order of $\mathcal{A}L_i/V_0$, we obtain the work done in the whole process as

$$W = \sum_{i=1}^M \left[\frac{nRT_e v_i \delta\tau}{V_0/\mathcal{A} - L_i} + \frac{\gamma nRT_e}{2} \left(\frac{v_i \delta\tau}{V_0/\mathcal{A} - L_i} \right)^2 \right] \quad (\text{S19})$$

$$\approx \frac{nRT_e \mathcal{A}}{V_0} \sum_{i=1}^M v_i \delta\tau \left(1 + \frac{\mathcal{A} L_i}{V_0} \right) + \frac{\gamma nRT_e}{2V_0^2} \sum_{i=1}^M (v_i \delta\tau)^2 \quad (\text{S20})$$

$$= \frac{nRT_e \mathcal{A}}{V_0} \sum_{i=1}^M v_i \delta\tau + \frac{nRT_e \mathcal{A}^2}{V_0^2} \sum_{i=1}^M v_i \delta\tau \sum_{j=1}^i v_j \delta\tau + \frac{\gamma nRT_e \mathcal{A}^2}{2V_0^2} \sum_{i=1}^M (v_i \delta\tau)^2 \quad (\text{S21})$$

$$= \frac{nRT_e \mathcal{A}}{V_0} \sum_{i=1}^M v_i \delta\tau + \frac{nRT_e \mathcal{A}^2}{V_0^2} \left[\left(\sum_{i=1}^M v_i \delta\tau \right)^2 - \sum_{i=1}^M (v_i \delta\tau)^2 \right] + \frac{\gamma nRT_e \mathcal{A}^2}{2V_0^2} \sum_{i=1}^M (v_i \delta\tau)^2 \quad (\text{S22})$$

$$= \frac{nRT_e \mathcal{A} L_M}{V_0} + \frac{nRT_e \mathcal{A}^2 L_M^2}{V_0^2} + \frac{(\gamma - 1) nRT_e \mathcal{A}^2}{2V_0^2} \sum_{i=1}^M (v_i \delta\tau)^2 \quad (\text{S23})$$

$$= \frac{nRT_e (V_f - V_0)}{V_0} + \frac{nRT_e (V_f - V_0)^2}{V_0^2} + \frac{(\gamma - 1) nRT_e (V_f - V_0)^2}{2V_0^2} \frac{\sum_{i=1}^M (v_i)^2}{\left(\sum_{i=1}^M v_i \right)^2}. \quad (\text{S24})$$

Here, $L_M = \delta\tau \sum_{i=1}^M v_i$ and $V_f - V_0 = \mathcal{A} L_M$ are respectively the total displacement of the piston and the change of the gas volume in the whole process. Note that the first two terms of Eq. (S24) is just the Taylor's expansion of the work done in quasi-static isothermal process $W_q = -nRT_e \ln(V_f/V_0)$ up to $(\Delta V/V_0)^2$. Consequently, the irreversible work $W^{(\text{ir})} = W - W_q$ is given by

$$W^{(\text{ir})} = \frac{(\gamma - 1) nRT_e (V_f - V_0)^2}{2V_0^2} \frac{\sum_{i=1}^M (v_i)^2}{\left(\sum_{i=1}^M v_i \right)^2} \quad (\text{S25})$$

$$= \frac{(\gamma - 1) P_0 (V_f - V_0)^2 \langle v^2 \rangle}{2M V_0 \langle v \rangle^2} \quad (\text{S26})$$

where $\langle v^2 \rangle = \left[\sum_{i=1}^M v_i^2 \right] / M$, and $\langle v \rangle = \left(\sum_{i=1}^M v_i \right) / M$. With the definitions $\Lambda \equiv \langle v^2 \rangle / \langle v \rangle^2$, and $\Theta \equiv P_0 (V_f - V_0)^2 / (2V_0)$, the irreversible work in discrete isothermal process of Eq. (6) in the main context is obtained.

IV. ADDITIONAL RESULTS FROM PRESSURE SENSORS S2 AND S3

In addition to the experimental data from pressure sensor S1 in the main context, we show the results from the pressure sensor S2 and S3 as following in Figures S3, and S4. These figures illustrate mainly the data at the temperature at $T_e = 313.15\text{K}$. Similar figures for $T_e = 323.15\text{K}$ can be obtained upon request.

* hdong@gscaep.ac.cn

[S1] B. Andresen, R. S. Berry, A. Nitzan, and P. Salamon, *Phys. Rev. A* **15**, 2086 (1977).

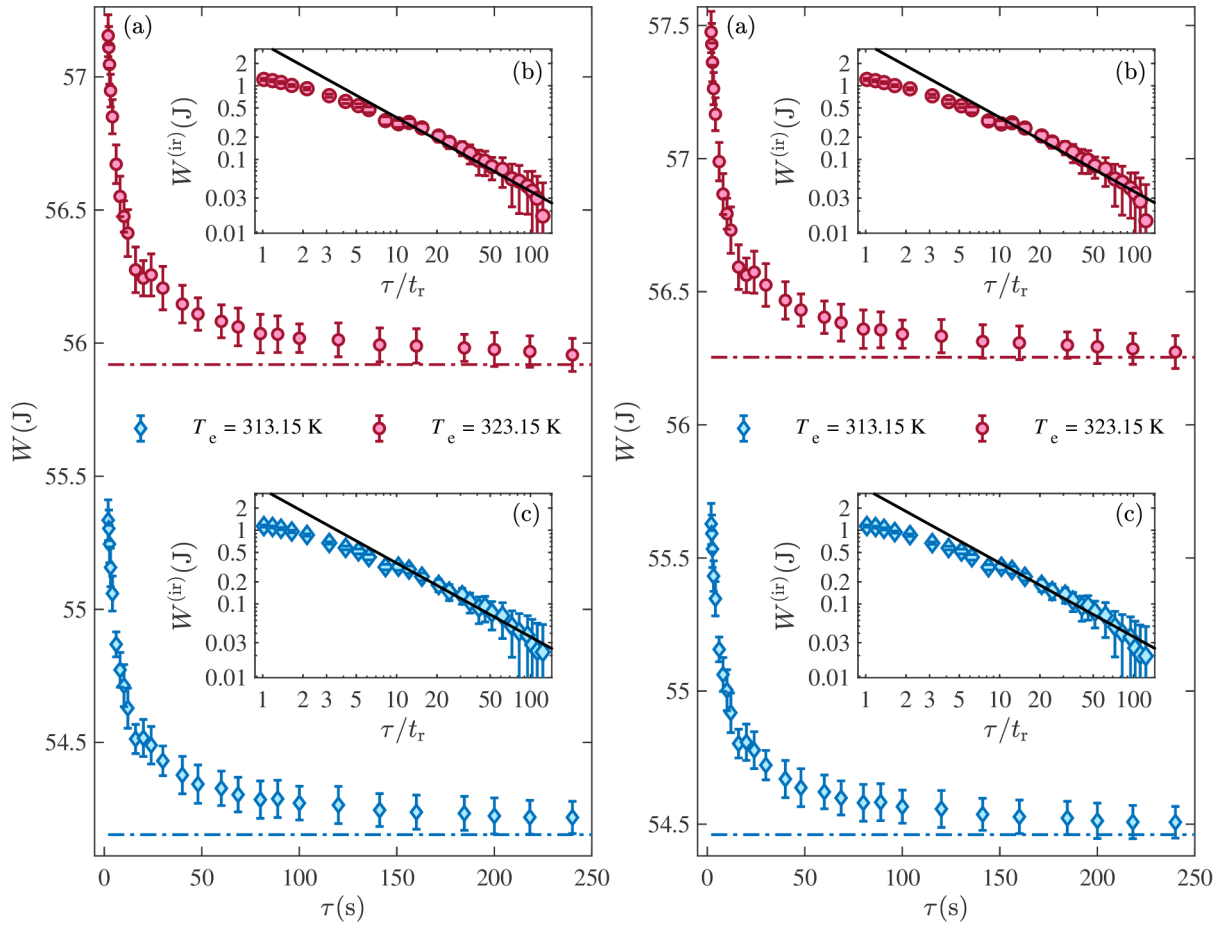


Figure S3. The irreversible work measured in the linear control scheme with sensors S2 (left panel) and S3 (right panel).

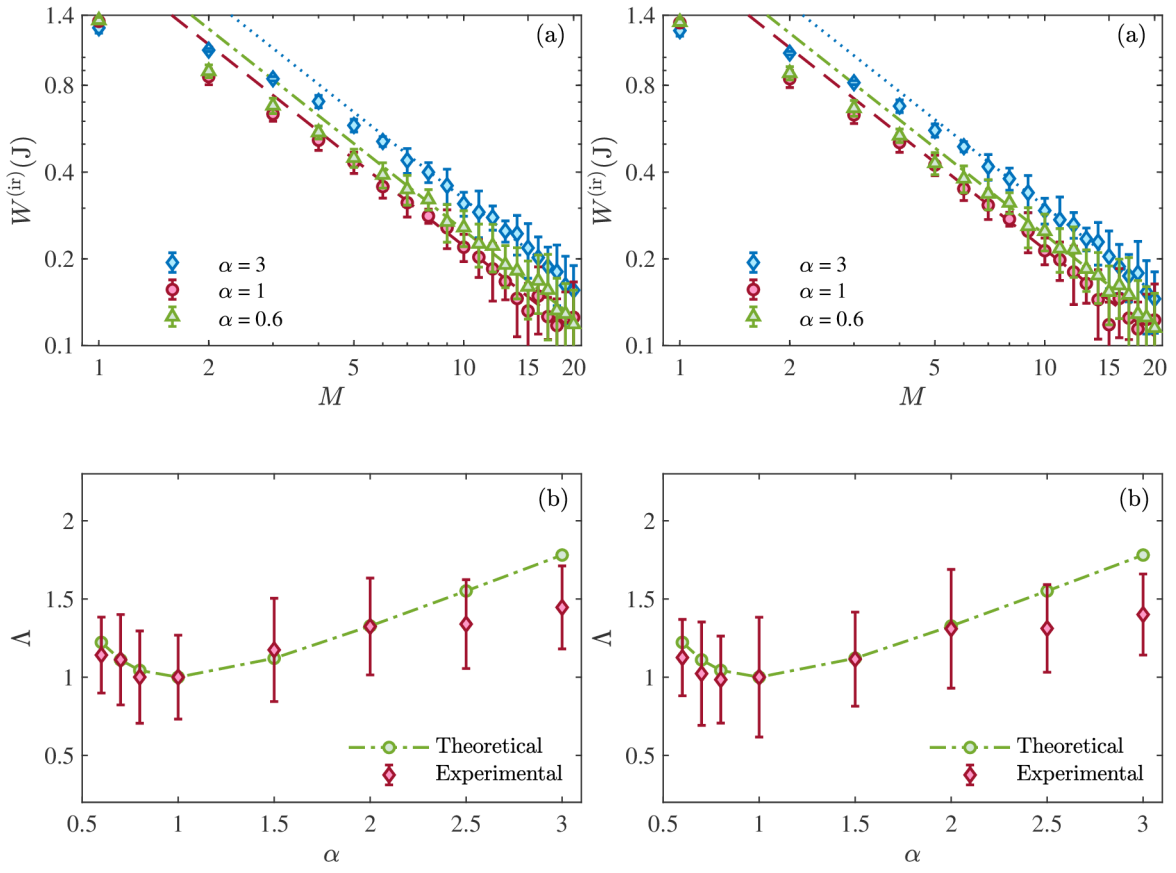


Figure S4. The irreversible work for the discrete process and the coefficient Λ estimated from experimental data with sensors S2 (left panel) and S3 (right panel) at temperature $T_e = 313.15\text{K}$.